


## Editor's Choice

# A Dose-Response Study of a Novel Method of Selective Tissue Modification of Cellular Structures in the Skin With Nanosecond Pulsed Electric Fields

David Kaufman, MD,<sup>1</sup> Michelle Martinez, RN, SSN,<sup>1</sup> Lauren Jauregui, BS,<sup>2</sup> Edward Ebberts, BAA, MBA,<sup>2</sup> Richard Nuccitelli, PhD,<sup>1</sup> <sup>2\*</sup> William A. Knappe, BS,<sup>2</sup> Darrin Uecker, MS,<sup>2</sup> and Darius Mehregan, MD<sup>3</sup>

<sup>1</sup>Kaufman and Davis Plastic Surgery, 1841 Iron Point Road, Folsom, California 95630

<sup>2</sup>Pulse Biosciences Inc., 3957 Point Eden Way, Hayward, California 94545

<sup>3</sup>Department of Dermatology, Wayne State University, 42 W. Warren Ave., Detroit, Michigan 48202

**Background and Objectives:** This study describes the effects of nanosecond pulsed electric fields (nsPEF) on the epidermis and dermis of normal skin scheduled for excision in a subsequent abdominoplasty. nsPEF therapy applies nanosecond pulses of electrical energy to induce regulated cell death (RCD) in cellular structures, with negligible thermal effects. Prior pre-clinical studies using nsPEF technology have demonstrated the ability to stimulate a lasting immune response in animal tumor models, including melanoma. This first-in-human-use of nsPEF treatment in a controlled study to evaluate the dose-response effects on normal skin and subcutaneous structures is intended to establish a safe dose range of energies prior to use in clinical applications using nsPEF for non-thermal tissue modification.

**Study Design/Materials and Methods:** Seven subjects with healthy tissue planned for abdominoplasty excision were enrolled. Five subjects were evaluated in a longitudinal, 60-day study of effects with doses of six nsPEF energy levels. A total of 30 squares of spot sizes 25mm<sup>2</sup> or less within the planned excision area were treated and then evaluated at 1 day, 5 days, 15 days, 30 days, and 60 days prior to surgery. Photographs were taken over time of each treated area and assessed by three independent and blinded dermatologists for erythema, flaking and crusting using a 5-point scale (0 = low, 4 = high). Punch biopsies of surgically removed tissue were processed and evaluated for tissue changes using hematoxylin and eosin, trichome, caspase-3, microphthalmia transcription factor, and elastin stains and evaluated by a dermatopathologist. The skin of two subjects received additional treatments at 2 and 4 hours post-nsPEF and was evaluated in a similar manner.

**Results:** Most energy settings exhibited delayed epidermal loss followed by re-epithelization by day 15 and a normal course of healing. Histologic analysis identified the appearance of activated caspase-3 at two and four hours after nsPEF treatment, but not at later time points. At the 1-day time point, a nucleolysis effect was observed in epidermal cells, as evidenced by the lack of nuclear staining while the epidermal plasma membranes were still intact. Cellular structures within the treatment zone such as melanocytes, sebaceous glands, and hair follicles

were damaged while acellular structures such as elastic fibers and collagen were largely unaffected except for TL6 which showed signs of dermal damage. Melanocytes reappeared at levels comparable with untreated controls within 1 month of nsPEF treatment.

**Conclusions:** The selective effect of nsPEF treatment on cellular structures in the epidermal and dermal layers suggests that this non-thermal mechanism for targeting cellular structures does not affect the integrity of dermal tissue within a range of energy levels. The specificity of effects and a favorable healing response makes nsPEF ideal for treating cellular targets in the epidermal or dermal layers of the skin, including treatment of benign and malignant lesions. nsPEF skin treatments provide a promising, non-thermal method for treating skin conditions and removing epidermal lesions. © 2019 The Authors. *Lasers in Surgery and Medicine* Published by Wiley Periodicals, Inc.

**Key words:** nanosecond; nanosecond pulsed electric fields (nsPEF); pulses of energy; cellular target; abdominoplasty; histology; regulated cell death; immunogenic cell death; caspase-3; danger-associated molecular patterns (DAMPs)

## INTRODUCTION

Nanosecond pulsed electric fields (nsPEF) have been applied to many different biological systems over the past

This is an open access article under the terms of the Creative Commons Attribution-NonCommercial-NoDerivs License, which permits use and distribution in any medium, provided the original work is properly cited, the use is non-commercial and no modifications or adaptations are made.

Conflict of Interest Disclosures: All authors have completed and submitted the ICMJE Form for Disclosure of Potential Conflicts of Interest and have disclosed the following: LJ, EE, RN, WK, and DU are employed by Pulse Biosciences Inc., the company that fabricated the pulse generator used in this study.

\*Correspondence to: Richard Nuccitelli, PhD, Pulse Biosciences, 3957 Point Eden Way, Hayward, CA 94545. E-mail: rnuccitelli@pulsebiosciences.com

Accepted 15 July 2019

Published online 2 August 2019 in Wiley Online Library

(wileyonlinelibrary.com).

DOI 10.1002/lsm.23145

two decades [1]. These pulses are so short that they have the unique ability to penetrate into cells and organelles before charge rearrangements can respond to neutralize the imposed field. This electric field penetration can “stimulate” many different cellular responses as varied as secretion [2,3], differentiation [4], and regulated cell death (RCD) [5], depending on the amount of energy applied and cell type treated. The form of nsPEF applied in this study was tuned to deliver is a non-thermal signal to induce RCD within a localized treated area determined by the placement of a treatment tip with two rows of bipolar microneedles. The cell-specific nsPEF mechanism avoids damage to acellular tissue components mainly because it is non-thermal due to the low energy and ultrashort pulses used [6,7]. This is in contrast with other common treatments, such as laser resurfacing, electrocauterization, and cryotherapy, whose primary mechanism of action is thermal necrosis [8] with skin effects visible almost immediately. Rather than heating the skin, nsPEF therapy generates nanopores in intracellular organelles to stimulate RCD. This results in a signaling cascade leading to apoptotic cell death in which the treated epidermis slowly dies over a day and within a week is replaced by a regenerated epidermis without any changes in the underlying dermal fibers. Extensive pre-clinical work on animal models has demonstrated that this results in a favorable, scarless healing profile as well as a broad systemic and sustained antitumor immune response to malignant lesions [9–15]. Thus, nsPEF has a potential dual effect in malignant cells of eliminating tumor cells via an RCD mechanism, followed by a systemic immune response triggered by the immune system’s detection of antigens that are released during RCD. Extensive pre-clinical research by several investigators has revealed that the RCD signaling cascade initiated by nsPEF includes increases in intracellular calcium [16,17] reactive oxygen species [18,19], caspase-3 activation [10,11], and the initiation of DNA fragmentation [20].

The main goals of this study are to characterize the clinical and histological effects of a range of energy settings for nsPEF on human skin and to document the time course of histological changes in the treated regions. A secondary goal is to detect the activation of caspase-3 as an indicator of the RCD pathway observed in pre-clinical models.

## METHODS

### Study Design

The study was designed to meet two objectives: (i) to establish a range of nsPEF exposure that could be delivered safely to healthy human tissue with predictable damage to the skin with associated predictable recovery, and (ii) to perform a histological analysis of the nsPEF-treated tissue to correlate clinical recovery scores and images with histology scores and observations for the respective six energy levels tested.

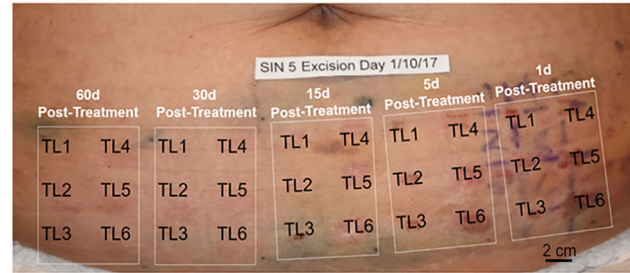


Fig. 1. Photographic representation of the treatment grid of a single subject. Total grid consists of five smaller grids for each time interval post-nanosecond pulsed electric fields (nsPEF) treatment. Each smaller time interval grid contains six identical treatment sites in which the same six nsPEF treatment levels (TLs) were applied. The result is 30 treatment sites at five different time intervals pre-abdominoplasty for each patient

Study objectives were achieved by treating healthy abdominal skin in pre-defined grid patterns at six different energy treatment levels (TLs) (Fig. 1). The treated skin was normal abdominal epidermis and dermis that was planned for removal in an elective cosmetic abdominoplasty procedure. nsPEF treatments were performed in the pre-arranged grid over a scheduled time period such that at the time of abdominoplasty, the nsPEF-treated areas would correspond to a range of time intervals post-treatment, resulting in a longitudinal time series of treated skin samples.

The degree of effect of the various energy TLs was assessed by evaluating the clinical appearance and histologic response of each treatment region. The time course of the wound response and the degree of injury were evaluated through histologic examination and scored evaluation of samples collected on the day of surgery representing 1, 5, 15, 30, and 60 days post-nsPEF treatment, and by a blinded assessment of the photographic appearance of epidermis through a validated scoring scale for each treated site over the same time intervals.

### Subjects

Biomedical Research Institute of America IRB reviewed the proposed study plan and provided oversight for this Non-Significant Risk study. All subjects provided written informed consent and the study conforms to the US Federal Policy for the Protection of Human Subjects.

For the main aim of this study, an initial cohort of five subjects was screened and enrolled by the principle investigator from patients already scheduled to undergo elective abdominoplasty surgery. Subjects presented with healthy abdominal skin, a normal range of skin laxity and no history of skin treatments on the abdomen. All subjects were females with an average age of 50 years (standard deviation: 14; range: 29–64 years). Two subjects were White and three were Hispanic. One subject had three prior Cesarean deliveries and one other subject had a previous cholecystectomy. Preexisting surgical scars were not present in skin areas identified for treatment. Twenty

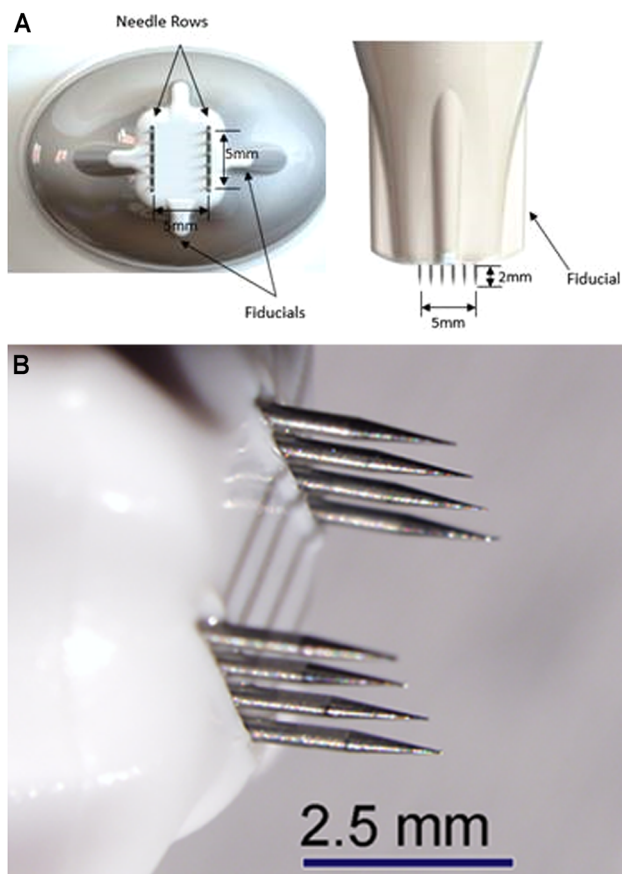


Fig. 2. Applicator tips used. (A) 5 × 5 mm tip and (B) 2.5 × 2.5 mm tip

percent of subjects were rated as Fitzpatrick skin type II-tans minimally, 60% were Type III-tans uniformly and 20% were type IV-moderate brown. Prior to treatment, striae were observed in three of the five subjects.

### Treatment

Six nsPEF energy levels were evaluated in the initial cohort of five patients enrolled in a 60-day longitudinal study. For each of the five patients, a central area corresponding to the planned resection zone was divided into five identical large grids, with each large grid element corresponding to the study time interval (60 days, 30 days, 15 days, 5 days, and 1 day post-nsPEF treatment). Each grid was further subdivided into six smaller square grids in order to designate the position for each energy TL, TL1–6. At the first treatment visit, tattoo marks were placed in the corners of each treatment-day grid guided by a thin plastic overlay as shown in Figure 1. Treatment areas were then demarcated on the skin on each treatment day using the plastic overlay and medical-grade ink. The treatment tips used for the 5 × 5 mm and 2.5 × 2.5 mm applicators used microneedles that were 2 mm long (Fig. 2).

The second cohort of two patients was enrolled in order to collect 2- and 4-hour time points. They had the same six

**TABLE 1. Summary of Pain Scores on Scale of 0 (Low) to 10 (High)**

	TL1	TL2	TL3	TL4	TL5	TL6
Average pain score	0.0	0.2	0.0	0.4	0.4	0.4
Highest pain score	0	4	0	4	7	3

treatment zones, and in addition to the 5 × 5 mm tip, some larger tips were tested to provide pilot data.

Treatments were performed using the nsPEF generator manufactured by Pulse Biosciences. The system consists of (i) an electrical pulse generator that produces pre-determined sequences of high intensity nanosecond electrical energy pulses to skin, (ii) a hand-piece applicator held by the clinician during application of nanosecond pulses to the skin surface, and (iii) a sterile, single-patient use treatment tip, which contains an array of electrically-conductive microneedles that penetrate into the skin with varying spot sizes.

Prior to treatments, 2% lidocaine injections were applied to facilitate patient comfort during energy delivery. All treatments were conducted by the same nurse who injected the same amount of lidocaine beneath each treatment spot. Two treatment tip spot sizes were tested in the study: The 2.5 × 2.5 mm treatment tip (TL1–3) and the 5.0 × 5.0 mm treatment tip (TL4–6). The same six discrete TLs were administered at each of the five time intervals per pre-marked grid. One cycle of an energy TL consisted of a single placement of a treatment tip on a square of tissue followed by a series of discrete electrical energy pulses of nanosecond durations contained within an overall pulsing sequence lasting less than 20 seconds. The TLs represented different amounts of nsPEF energy, where the number of pulses, applied voltage, pulse duration, and tip area combine to produce a particular TL. The total electrical energy for any treatment square ranged between 1 and 6 J, with an estimated total energy density range of 0.05–0.16 J/mm<sup>3</sup>.

### Photographic Assessment

Photographs were taken of all treatment sites defined by the pre-marked grids, for all subjects at each time point using both a (Sony RX100; Sony Corporation of America, New York, NY) and (Nikon D810; Nikon Inc., Melville, NY) with a (Micro AF-S 60 mm Lens; Nikon Inc), and (R1-C1 Flash System; Nikon Inc., Melville, NY) (using 3 flashes). At the completion of the study, photographic review image sets were prepared with a series of treatment site photos for the five longitudinal subjects across all time periods and TLs, with subject and treatment information masked. Qualified, independent reviewers were presented with a Rating Key for the photo evaluation along with a complete set of photos and instructed to rank each photo for erythema, flaking, and crusting using a defined 5-point rating scale. Both inter-rater and intra-rater reliability comparisons were



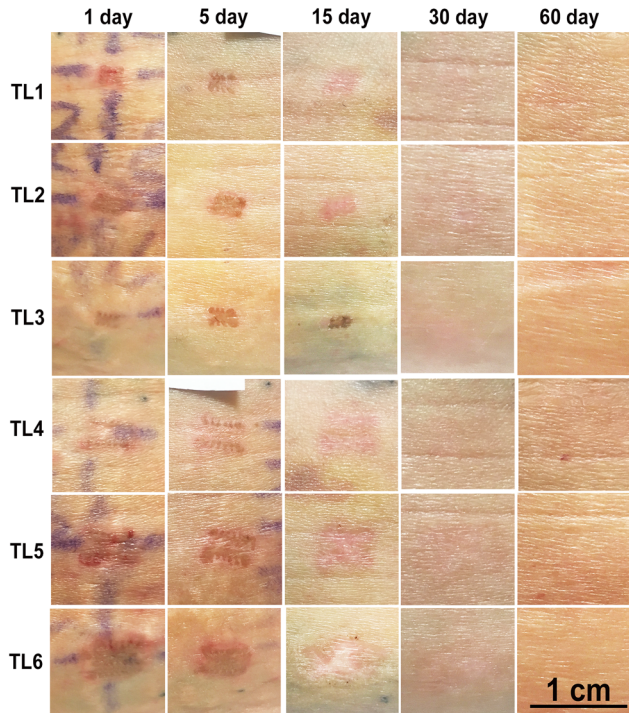


Fig. 3. Photographic montage of the treatment sites captured on 5 days on a single subject. Treatment levels increase in strength downwards (TL1 is the lowest level). Time elapsed since the treatment day increases left to right. Individual images represent areas that are approximately 1 cm wide

assessed to address any potential bias. The average rate of intra-rater agreement of outcomes that fell within one point at different time points was 94.6%. The overall inter-rater agreement was 92%, agreement defined as 2 out of 3 of the raters having an “exact match” in the measurement of each photograph.

**Histologic Sample Preparation**

The abdominal skin targeted for resection was excised, using the tattoo dots to recover original treatment

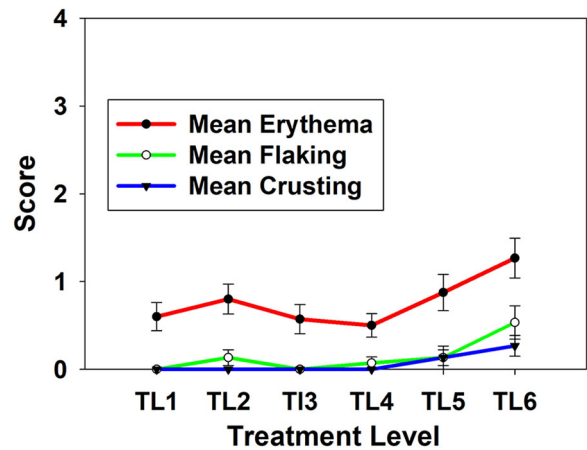


Fig. 4. Mean photographic assessment scores for the 60-day time point for all five initial patients. Error bars indicate standard error of the mean

locations of the five grids. An 8-mm punch was used to sample each treatment area, producing 30 full-thickness dermal samples, with two additional control samples just outside the treatment grids for each of the study subjects. In some cases, an area of skin with striae was biopsied along with normal control. Individual samples were placed in collection jars with 10% neutral formalin for preservation and shipped to a histopathology lab, Pinkus Dermatopathology Laboratory, for staining and evaluation by a dermatopathologist.

This investigation was intended as a small safety and proof-of-concept study that was not designed for statistical hypothesis testing. The quantitative analysis performed represents the data generated from the samples available for histological analysis by the dermatopathologist.

**Histologic Examination**

Samples were bisected perpendicular to the epidermal surface to create full-thickness sections and were mounted to expose the epidermal and dermal cross-section. Hematoxylin and eosin staining preparations were made for all time points. Preparations were also made for selected time points

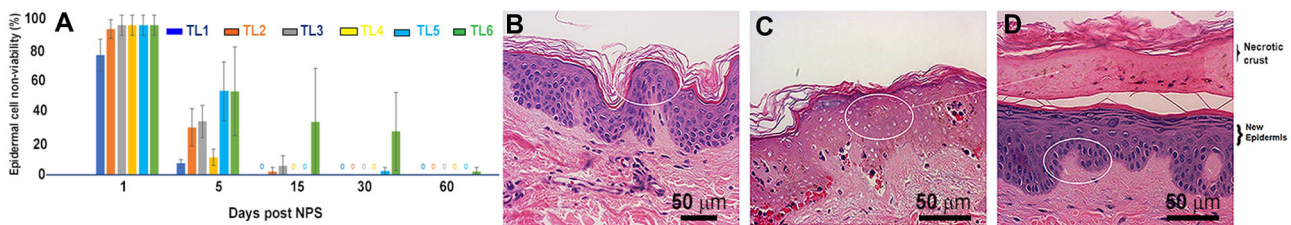


Fig. 5. Time course of epidermal viability loss and recovery. (A) Measure of epidermal non-viability for the five treatment levels over time. (B) Untreated control skin shows strong nucleus labeling in the epidermis (oval). (C) One day after TL3 nanosecond pulsed electric field (nsPEF) treatment; Oval marks nonviable epidermis that displays minimal inflammation and contains “ghost cells” with intact cell membranes with “hollow” nuclei that do not stain. (D) Day 7 post-treatment; necrotic epidermis from “C” has the appearance of a crust and is delaminating from the new epidermal layer (oval) that contains normally staining nuclei and minimal inflammation

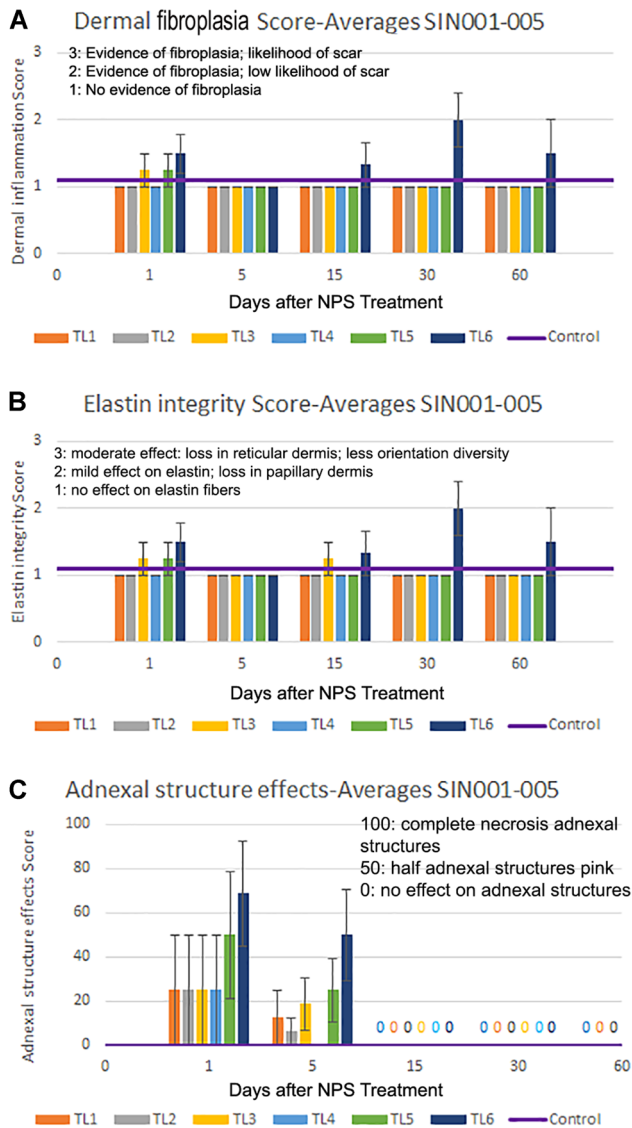


Fig. 6. Scoring for nanosecond pulsed electric field (nsPEF) treatment-induced changes in the dermis. (A) Dermal fibroplasia was minimal for all treatment levels except TL6. (B) Elastin integrity was not affected for all treatment levels except TL6. (C) Adnexal structures were affected on days 1 and 5 for TL5 and TL6 but recovered by day 15

using trichrome, elastic orcein Giemsa, microphthalmia transcription factor, and activated caspase-3 staining protocols. Samples prepared with these five protocols were examined by a board-certified dermatopathologist (DM) and graded using scoring methods designed to evaluate dermal inflammation, elastic fiber integrity, adnexal structure effects, melanocyte density, and the presence of activated caspase-3 as an immunogenic cell death marker. The assessment of melanocytes was performed by counting melanocytes identifiable in three randomly selected, 1-mm treatment zones of the sample and taking the average of the

three. All other scoring definitions did not rely on an actual density count.

## RESULTS

### Clinical Experience

Local lidocaine injections applied prior to the nsPEF treatment were effective in controlling discomfort as rated by the subjects using a standardized pain scale ranging from 0 to 10, 10 being the highest (Table 1). The average pain scores across all TLs reported by the five subjects ranged from 0 to 0.4. The highest pain scores ranged from 0 to 7 across the five subjects for levels TL1–TL6. Of note, the highest pain score reported was associated with a single subject at TL5, while all other patients scored a 0–2.

All wounds healed without exudate or significant discomfort to the patient. The treated skin healed as expected. No signs of infection were present, and no adverse events occurred.

### Photographic Assessment

The nsPEF-treated areas exhibit a normal wound healing profile. A representative photographic montage from one subject is shown in Figure 3. Localized epidermal damage and erythema is apparent 1-day post-treatment for all TLs in all subjects. Formation of eschar is evident 5 days post-treatment. Sites treated at higher TLs appeared more affected, with the highest TL sites (TL6) associated with clear localized erythema and eschar formation 5 and 15 days after nsPEF treatment. Epidermal recovery appears complete by 30 days. At 60 days post-treatment, slightly higher erythema scores for the two highest energy levels indicated a longer healing time (Figs. 3 and 4). Moderate erythema was mostly resolved by study end, with TL5–6 sites exhibiting some erythema up to day 60. Epidermal scale and inflammatory cell crust formation was low for TL1–4 and resolved by day 60 for TL1–5. The formation of an eschar was modest and was greatest for TL6. The clinical evaluation was consistent with the histological findings.

### Histological Findings

The time sequence of histopathology micrographs depicts a typical evolution of the wound creation and healing response to nsPEF exposure (Fig. 5). Normal, untreated skin exhibits healthy epidermis with intact rete ridges. One-day post-nsPEF treatment, the epidermis appears nonviable with evidence of “ghost cells” which appear to have intact cellular membranes and pale-staining nuclei (Fig. 5C). The epidermis was assessed as generally nonviable for the complete epidermal thickness at 1-day post-treatment for all TLs in all subjects, showing an average of 90% nonviable cells across the six TLs evaluated (Fig. 5A). Samples observed 5 days post-treatment showed epidermal recovery in the formation of a new epidermal layer beneath the necrotic epidermal crust (Fig. 5D). By 15 days of post-nsPEF treatment, the



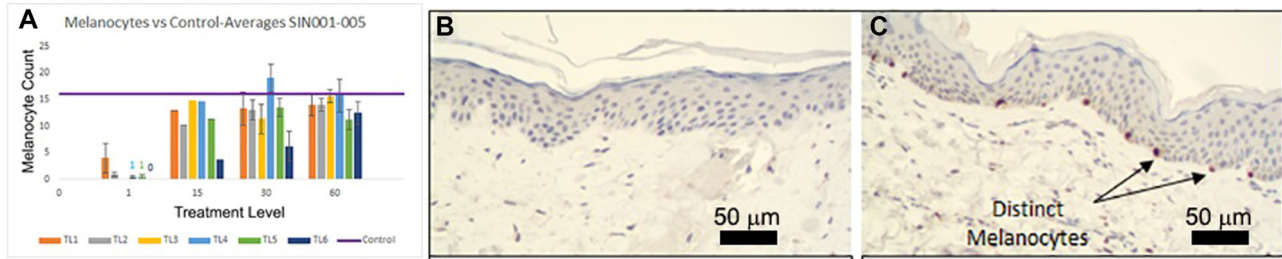


Fig. 7. Mean melanocyte count using microphthalmia transcription factor (MITF) immunostaining. (A) Time course of recovery for five different treatment levels. (B) Immunohistochemistry (IHC) using MITF on section 15 days after TL3 treatment. (C) MITF IHC 60 days after TL3 treatment

epidermis had returned to a normal thickness in almost all samples.

A dermatopathologist scored the histological specimens for different indicators of epidermal effects, dermal injury, fibroplasia, elastin fiber integrity, and adnexal structure integrity (Fig. 6). No evidence of injury to dermal collagen, as indicated by more aligned and flattened collagen fibers in the dermis, was observed in tested samples. The number of dermal fibroblasts observed was reduced at 1 and 5 days post-treatment and by 15 days post-treatment had recovered to density levels comparable with control samples. A small degree of dermal fibroplasia was observed after treatment (1, 15, and 30 days post-treatment) presenting as horizontal new collagen deposition with loss of papillary dermal elastic fibers. Dermal fibroplasia scores were generally very low, with average scores close to scores from control samples for most time points and most TLs, except for TL6 (Fig. 6A). Some samples from TL5 and TL6 sites exhibited focal papillary dermal necrosis, which was observed at days 1 and 5 but not on day 15 or later. In two patients, treatments at TL6 resulted in some parallel fibrosis of dermal collagen bundles at 30 days and epidermal necrosis was followed by a formation of an inflammatory eschar. This formation healed by 60 days with some epidermal flattening and minimal papillary dermal fibrosis.

Elastic tissue appeared intact in most samples. For the larger treatment tip, a slight decrease in elastic fiber presence was occasionally noted for TL6 samples on day 30 with normal elastic fibers observed on the other days sampled (Fig. 6B).

Adnexal structures in the dermis such as sebaceous glands, eccrine ducts, and hair follicles were affected by all TLs on day 1 but recovered by day 15 (Fig. 6C). There was a partial to full necrosis of these structures at level TL5 and TL6, but this did not cause permanent elimination of these structures. By 60 days of post-nsPEF treatment, the epidermis, hair follicles, and eccrine glands all appeared normal, except for one patient sample at TL6.

A nearly complete but temporary loss of melanocytes is observed in the treatment zone post-treatment (Fig. 7). By 30 days of post-nsPEF treatment, most treatment sites showed a regenerated epidermis with a significant rebound in melanocyte density

### Caspase-3 Activation

One of the indicators of RCD is the appearance of activated caspases which are a family of protease enzymes that play an essential role in the apoptosis pathway. Caspase-3 is considered an executor caspase in this family and once activated it hydrolyzes cytoplasmic proteins. It is

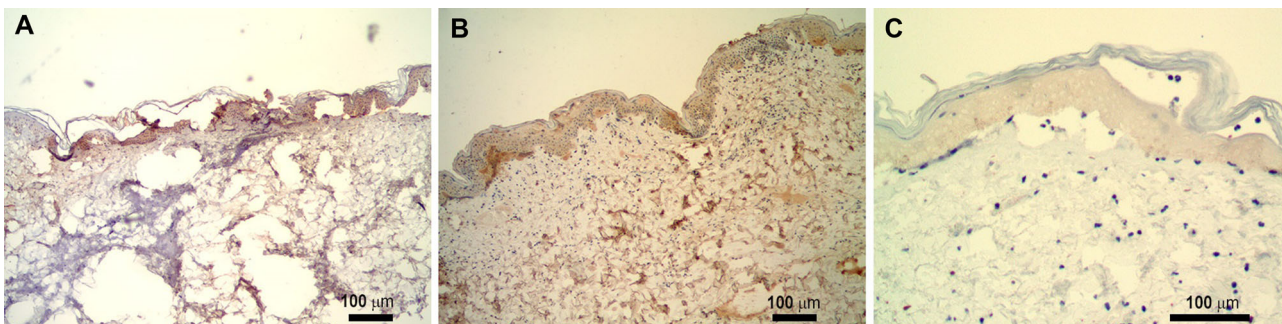


Fig. 8. Immunohistochemical labeling of nanosecond pulsed electric field (nsPEF)-treated skin section with antibody to activated caspase-3 (brown stain). (A) Two hours post-nsPEF treatment, (B) 4 hours post-nsPEF, and (C) 24 hours post-nsPEF

known to be involved in the early hours of the RCD pathway but generally is not detected at later times [10,11]. In order to study these earlier time points, two additional subjects were subsequently added under a similar protocol and treatment parameters. The samples were stained using the same method as the initial five patients and evaluated by the same dermatopathologist. Histologic analysis showed that active caspase-3 is detected at both 2 and 4 hours post-nsPEF treatment for all treatment tips evaluated (Fig. 8) but no activity was detected for any later time points.

## DISCUSSION

### Clinical and Histological Findings

Histologic examination showed a minimal degree of epidermal and dermal inflammation associated with nsPEF treatments that was smaller than typically observed in skin treated with thermal or other physical methods of epidermal lesion removal [21]. There was also no evidence of thermal injury such as denatured collagen. This lack of thermal effect is consistent with earlier work using similar treatment parameters to treat model melanoma tumors in mice using sub-Joule nsPEF doses which results in temperature rises of approximately 3°C [6,7]. The low dermal fibroplasia scores noted for TL1–5 are suggestive of a low likelihood of future scar formation. The observation that some samples showed focal perivascular inflammation with fibrin deposition appeared to have no clinical correlation to the degree of epidermal necrosis or wound healing. Dermal return of the fibroblast densities after day 15, suggests recovery of fibroblasts and associated normal capacity to rebuild connective dermal tissue, especially for TL1–5. Elastic fibers remained largely intact, with small decreases in elastic fiber integrity for TL4–6. The return of elastic fiber integrity to control levels by study end and the modest alteration of collagen is predictive of normal healing and minimal scarring.

Melanocyte recovery was rapid, with pigment cell density returning to levels comparable with controls within 1 month (Fig. 7). Such a recovery is consistent with normalization of skin pigmentation over time and is predictive of normal melanin production and eventual normalization of skin pigment. The recovery of hair follicles and eccrine glands was also indicative of a complete epidermal and dermal healing response for all TLs except TL6.

### Mechanism

The histologically observed effect on the cellular structures including epidermal cells, hair follicles, and eccrine ducts exemplifies the cell-specific mechanism of the nsPEF treatment. To further examine the method in which cell death occurs, immunohistochemical stains for active caspase-3, an early marker of RCD, were performed and this enzyme was detected at 2 and 4 hours post-nsPEF application. It is possible that the “ghost cells” exhibited within 24 hours after nsPEF treatment are a

product of this early activation of caspase-3. This is the first evidence that nsPEF therapy activates caspase-3 in humans, confirming prior results observed in pre-clinical study models.

We conclude that nsPEF therapy delivers ultrashort pulses of non-thermal electrical energy to the skin that can initiate RCD in cellular components of the epidermis and dermis with little or no effect on the fibrillar components. This new modality provides a novel method to selectively eliminate unwanted cellular lesions in the skin with very short treatment times and with little to no scarring. Clinical trials are underway to explore possible applications of nsPEF for the treatment of seborrheic keratosis, sebaceous gland hyperplasia, warts, acne, and other skin lesions.

## ACKNOWLEDGMENTS

The authors thank our blinded reviewers of the photos of the treatment areas: Girish Munavalli MD, Victor Ross MD, James Newman MD, Adele Haimovic MD, and Melba Herrera MD.

## REFERENCES

- Schoenbach KH. Bioelectric effect of intense nanosecond pulses. In: Pakhomov AG, Miklavcic D, Markov MS, editors. *Advanced Electroporation Techniques in Biology and Medicine, Biological Effects of Electromagnetics*. Boca Raton, FL: Taylor and Francis Group; 2010. pp 19–50.
- Zhang J, Blackmore PF, Hargrave BY, Xiao S, Beebe SJ, Schoenbach KH. Nanosecond pulse electric field (nanopulse): A novel non-ligand agonist for platelet activation. *Arch Biochem Biophys* 2008;471(2):240–248.
- Hargrave B, Li F. Nanosecond pulse electric field activation of platelet-rich plasma reduces myocardial infarct size and improves left ventricular mechanical function in the rabbit heart. *J Extra Corpor Technol* 2012;44(4):198–204.
- Bai F, Gusbeth C, Frey W, Nick P. Nanosecond pulsed electric fields trigger cell differentiation in *Chlamydomonas reinhardtii*. *Biochim Biophys Acta Biomembr* 2017;1859(5):651–661.
- Nuccitelli R, McDaniel A, Anand S, et al. Nano-pulse stimulation is a physical modality that can trigger immunogenic tumor cell death. *J Immunother Cancer* 2017;5:32.
- Nuccitelli R, Pliquett U, Chen X, et al. Nanosecond pulsed electric fields cause melanomas to self-destruct. *Biochem Biophys Res Commun* 2006;343(2):351–360.
- Pliquett U, Nuccitelli R. Measurement and simulation of Joule heating during treatment of B-16 melanoma tumors in mice with nanosecond pulsed electric fields. *Bioelectrochemistry* 2014;100:62–68. <https://doi.org/10.1016/j.bioelechem.2014.03.001>
- Orringer JS, Rittie L, Baker D, Voorhees JJ, Fisher G. Molecular mechanisms of nonablative fractionated laser resurfacing. *Br J Dermatol* 2010;163(4):757–768.
- Nuccitelli R, Tran K, Lui K, et al. Non-thermal nanoelectroablation of UV-induced murine melanomas stimulates an immune response. *Pigment Cell Melanoma Res* 2012;25: 618–629.
- Chen R, Sain NM, Harlow KT, et al. A protective effect after clearance of orthotopic rat hepatocellular carcinoma by nanosecond pulsed electric fields. *Eur J Cancer* 2014;50(15): 2705–2713.
- Nuccitelli R, Berridge JC, Mallon Z, Kreis M, Athos B, Nuccitelli P. Nanoelectroablation of murine tumors triggers a CD8-dependent inhibition of secondary tumor growth. *PLoS One* 2015;10(7):e0134364.
- Skeate JG, Da Silva DM, Chavez-Juan E, Anand S, Nuccitelli R, Kast WM. Nano-pulse stimulation induces immunogenic cell death in human papillomavirus-transformed tumors and

- initiates an adaptive immune response. *PloS one* 2018; 13(1):e0191311.
13. Guo S, Jing Y, Burcus NI, et al. Nano-pulse stimulation induces potent immune responses, eradicating local breast cancer while reducing distant metastases. *Int J Cancer* 2018;142(3):629–640.
  14. Guo S, Burcus NI, Hornef J, et al. Nano-pulse stimulation for the treatment of pancreatic cancer and the changes in immune profile. *Cancers* 2018;10(7):217.
  15. Lassiter BP, Guo S, Beebe SJ. Nano-pulse stimulation ablates orthotopic rat hepatocellular carcinoma and induces innate and adaptive memory immune mechanisms that prevent recurrence. *Cancers* 2018;10(3):E69.
  16. Vernier PT, Sun Y, Marcu L, Salemi S, Craft CM, Gundersen MA. Calcium bursts induced by nanosecond electric pulses. *Biochem Biophys Res Commun* 2003;310(2):286–295.
  17. White JA, Blackmore PF, Schoenbach KH, Beebe SJ. Stimulation of capacitative calcium entry in HL-60 cells by nanosecond pulsed electric fields. *J Biol Chem* 2004; 279(22):22964–22972.
  18. Pakhomova ON, Khorokhorina VA, Bowman AM, et al. Oxidative effects of nanosecond pulsed electric field exposure in cells and cell-free media. *Archives Biochem Biophys* 2012;527:55–64.
  19. Nuccitelli R, Lui K, Kreis M, Athos B, Nuccitelli P. Nanosecond pulsed electric field stimulation of reactive oxygen species in human pancreatic cancer cells is  $\text{Ca}^{2+}$ -dependent. *Biochem Biophys Res Commun* 2013;435(4): 580–585.
  20. Nuccitelli R, Chen X, Pakhomov AG, et al. A new pulsed electric field therapy for melanoma disrupts the tumor's blood supply and causes complete remission without recurrence. *Int J Cancer* 2009;125(2):438–445.
  21. Zelickson BD, Kist D, Bernstein E, et al. Histological and ultrastructural evaluation of the effects of a radiofrequency-based nonablative dermal remodeling device: A pilot study. *Arch Dermatol* 2004;140(2):204–209.